J Bionic Eng 16 (2019) 47–55
DOI: https://doi.org/10.1007/s42235-019-0005-8

Journal of Bionic Engineering
http://www.springer.com/journal/42235

Development of a Tactile and Slip Sensor with a Biomimetic Structure-enhanced Sensing Mechanism

Yonggang Jiang[1,2], Zhiqiang Ma[1], Bonan Cao[1], Longlong Gong[1], Lin Feng[1,2*], Deyuan Zhang[1]

1. *School of Mechanical Engineering and Automation*, *Beihang University*, *Beijing* 100191, *China*
2. *International Research Institute for Multidisciplinary Science*, *Beihang University*, *Beijing* 100191, *China*

Abstract

Tactile and slip sensors have gained tremendous attention for their promising applications in the fields of smart robotics, implantable medical devices and minimally invasive surgery. Inspired by the structure-enhanced sensing mechanisms of human fingertips and tree frog toes, we developed a tactile and slip sensor by combining biomimetic surface microstructures with highly sensitive P(VDF-TrFE) nanofiber sensors on a flexible polyimide substrate. As the surface microstructures could mediate the micro-vibration induced by slip motion, the frequencies of output signals revealed a strong correlation with the periods of microstructures. In addition, we proposed a method to discriminate touch force from slip motion using the criterion of standard deviation of time delay from the output signals of neighboring sensor elements.

Keywords: tactile sensor, slip detection, nanofiber, microstructure, biomimetic sensing

1 Introduction

Tactile sensing is of great significance in smart robotics, implantable medical devices and Minimally Invasive Surgery (MIS) instruments[1–3]. Minimally invasive surgery offers distinct advantages of small incisions, short recovery time, and less pain experienced by the patients compared to open surgery. However, because the MIS operating field is not directly accessed, surgeons face many difficulties in performing their operations through limited vision and impairing tactile perception. Herein, there is a strong demand to develop tactile and slip sensors for detection of grasper tissue interaction[4,5]. In addition, tactile sensors could also be used to feel hardness or tension of tissues, and to evaluate anatomical structures[6,7]. Currently, the transduction mechanisms of tactile sensors mainly include capacitive sensing[8,9], piezoelectric sensing[10–16], and piezoresistive sensing[17–19], transistor sensing[20] and opto-mechanical sensing[21,22]. New principle based on liquid metals[23] and electromagnetic inductions[24] were also reported.

Most of the existing tactile sensors are emphasized in touch force for grasping control, but slip detection is also crucial for operators to successfully manipulate tissues in minimally invasive surgery. In order to reduce the risk of minimally invasive surgery, we aim to develop a tactile and slip sensor for MIS forceps and get real-time information of whether the object is slipping so that operators can adjust the clamping force. Most point contact tactile sensors are incapable of discrimination between the slip motion and the touch force. A common approach is to use a sensor array with high spatial resolutions[25] by interpreting the deformation of contact surface. There are also some design examples of slip sensors using novel mechanisms. Francomano *et al.* reported a thermal slip sensor based on thermo-electrical phenomena[26]. As the movement of an object across the sensor will cause a high frequency and low amplitude vibration, micro-vibration-based slip detection using tactile sensors were well developed[27,28].

In human fingertips, the tactile perception is also mediated by skin vibrations generated as the finger scans the surface (Figs. 1a and 1b). When the sensor surface is patterned with parallel ridges mimicking the fingerprints, the spectrum of vibrations elicited by randomly textured substrates is dominated by one frequency set by the ratio of the scanning speed to the inter-ridge distance[29]. As

***Corresponding author:** Lin Feng
E-mail: linfeng@buaa.edu.cn

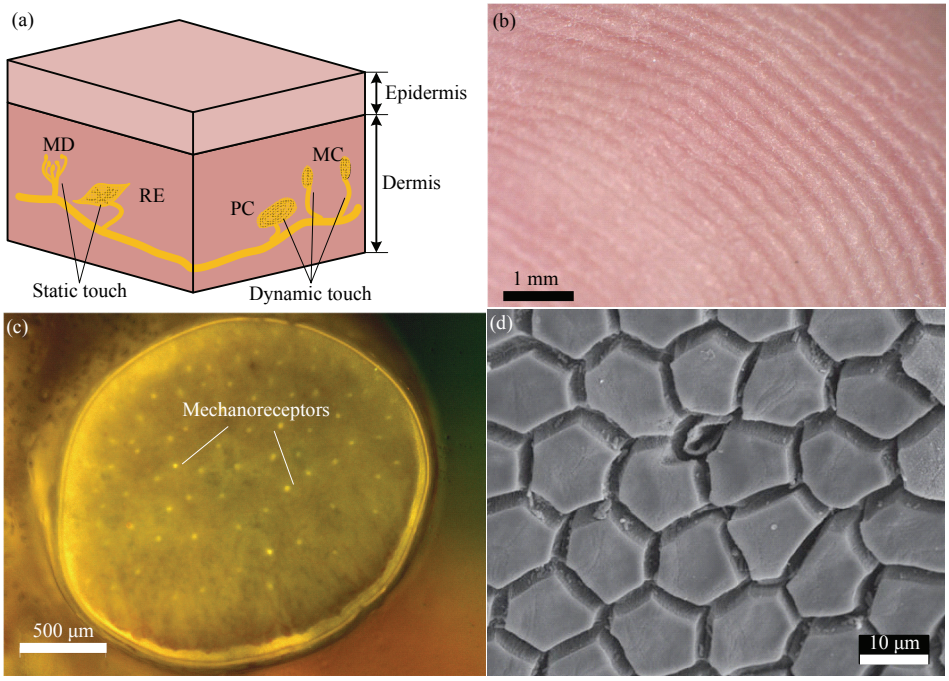

Fig. 1 Mechanoreceptors and surface structures of a human fingertip and a tree frog toe. (a) The structural and functional characteristics of human fingertips. Fingertip skin consists of slow-adapting mechanoreceptors [Merkel (MD) and Ruffini corpuscles (RE)] for static touch and fast-adapting mechanoreceptors [Meissner (MC) and Pacinian corpuscles (PC)] for dynamic touch. (b) Optical image of human fingerprints; (c) mechanoreceptors under the dermis of tree frog toes observed by fluorescence staining; (d) SEM images of the surface textures on the tree frog toes.

shown in Figs. 1c and 1d, the tree frog toes with complicated surface textures can not only increase the grasping force in wet interface[30], but also can detect slipping with the mechanoreceptors beneath the surface textures. Inspired by the structure-enhanced sensing mechanisms in nature, we presented a tactile and slip sensor by combining surface microstructures with piezoelectric polyvinylidene fluoride-trifluoroethylene (P(VDF-TrFE)) nanofiber web on a flexible Printed Circuit Board (PCB). Piezoelectric P(VDF-TrFE) nanofibers are used as the sensing materials for their high piezoelectric constants compared to P(VDF-TrFE) films or other flexible piezoelectric materials[31–33]. For instance, Persano *et al.* proposed a piezoelectric device based on P(VDF-TrFE) nanofibers, which could perform ultra-high sensitivity in extremely small pressure regime[33]. Microfabrication process makes it easy to be installed in the front of tiny surgical forceps. Surface microstructures on the sensor surface were proved to be able to enhance the ability to detect slipping information. By analyzing the signals from neighboring sensing elements, we could discriminate the slip motion with the touch force.

2 Design, fabrication and testing procedures

2.1 Design of the tactile and slip sensor

Inspired by the fine texture mediated tactile sensing mechanism of human fingertips and tree frog toes, we proposed a new principle of tactile and slip sensors as shown in Fig. 2. The sensor is composed of an elastic layer with microstructures, sensing elements embedded in the elastic layer, and a flexible PCB substrate. As shown in Fig. 2a, when the surface is stimulated with slip motion, it causes micro-vibrations of individual microstructures, which can be detected by the sensing elements. Given the spatial period of microstructures D and the relative slipping velocity v, the sensing elements will generate a signal with a frequency of $f = v/D$ as shown in Fig. 2b. In time domain, the output signals from the neighboring sensing elements show a very small time delay, which can be used to evaluate the direction of the slip motion as shown in Fig. 2c. In addition, when applied with periodical touch force instead of slip motion, the output signals of neighboring sensing elements will show no time delay. Therefore, this device is capable of detecting and discriminating tactile and slip

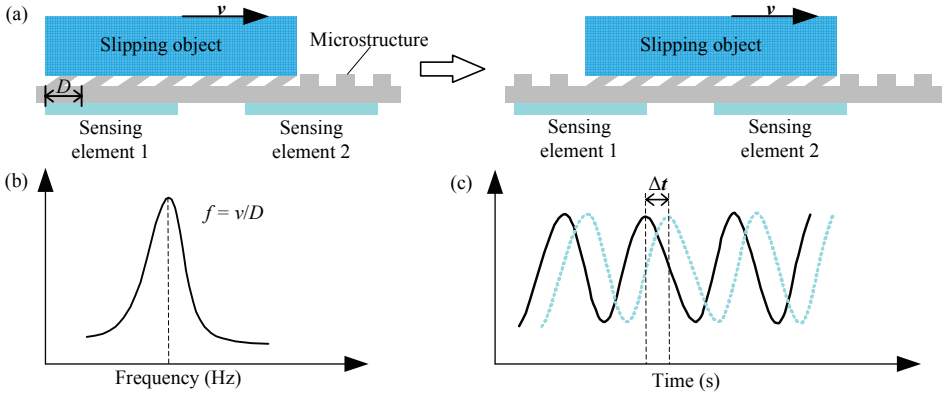

Fig. 2 Principle of slipping detection using piezoelectric sensors with bio-inspired surface microstructures. (a) Illustration of slipping interaction between object and sensors; (b) frequency spectrum of the sensor output; (c) time delay of output signals from neighboring sensing elements.

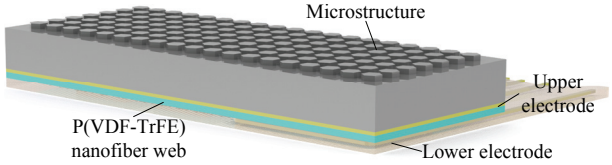

Fig. 3 Schematic structure of the tactile and slip sensor.

information.

The schematic structure of the tactile and slip sensor is illustrated in Fig. 3. Polydimethylsiloxane (PDMS) elastic layer with microstructures forms the interface of tactile and slip detection. Parallel ridged structures and hexagonal structures are used with the inspiration from the human fingertips and tree frog toes. At the bottom of the PDMS elastic layer, a P(VDF-TrFE) nanofiber web sandwiched by upper and lower electrodes forms the sensing element. The upper electrode is used for electrical ground, and the individual lower electrodes generate output signals.

2.2 Fabrication process

The stepwise fabrication process of the tactile and slip sensors is illustrated in Fig. 4. Firstly, flexible PCB was prepared with individual leads and plated gold lower electrodes (Fig. 4a). Secondly, a P(VDF-TrFE) nanofiber web was formed on the PCB using a far-field electrospinning method (Fig. 4b). The electrospinning process has been reported in detail in our previous works[31,32]. Thirdly, the upper electrode was formed by coating a layer of conductive resin (H20E, EPOTEK, USA) (Fig. 4c). The negative photoresist SU-8 was spin-coated onto the clean glass wafer at a speed of 1000 rpm for 45 s and the photoresist thickness was approximately 150 μm. The bio-inspired surface microstructures were patterned by photolithography to form the SU-8 mold. A liquid PDMS elastomer and a curing agent were mixed using a 10:1 ratio by weight. The degassed mixture was poured into the SU-8 mold, curing at 80 ˚C for 2 h finally peeled off as PDMS molds. Then, PDMS liquid was poured into the PDMS molds. After curing, the PDMS was peeled off from the molds and microstructures were formed. The parallel ridged microstructures with 200 μm and 400 μm widths were fabricated, and the interval between two adjacent microstructures was equal to the width. The hexagonal microstructures with 160 μm and 320 μm side lengths were developed. The center-to-center distance between two adjacent hexagonal microstructures was three times to their side lengths. Finally, the elastic layer was adhesively bonded with the sensing layer, and device was electrically wired for characterization (Fig. 4f).

The P(VDF-TrFE) nanofiber web with a thickness of 81 μm ± 3 μm was prepared by electrospinning as shown in Fig. 5a. The P(VDF-TrFE) nanofiber web shows high degrees of alignment as shown in Fig. 5b, and the average diameter of P(VDF-TrFE) nanofibers is approximately 500 nm. Figs. 5c and 5d illustrate the bio-inspired surface microstructures including parallel ridged microstructures and hexagonal microstructures for slipping detection. The height of the microstructures is approximately 150 μm. The fabricated tactile and slip sensor is illustrated in Fig. 6a, which can be assembled onto a surgical forcep as demonstrated in Fig. 6b.

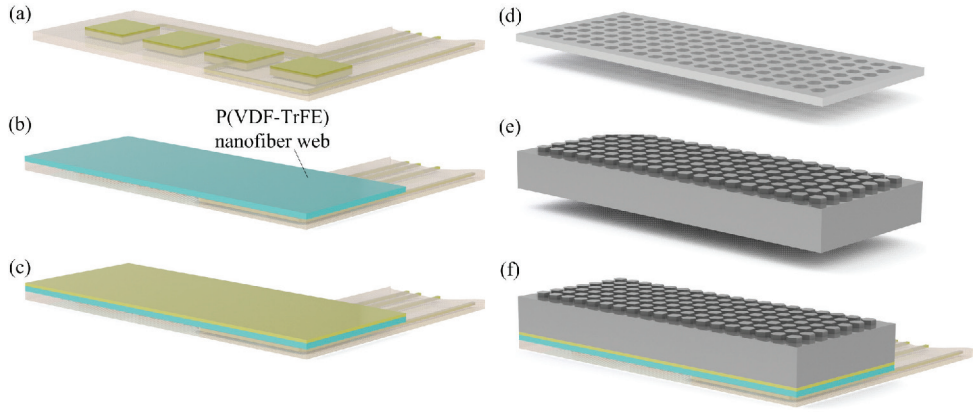

Fig. 4 Schematic illustration of the fabrication process. (a) Preparation of flexible PCB substrate with lower electrodes; (b) electrospinning of P(VDF-TrFE) nanofiber web; (c) coating conductive resin for the upper electrode; (d) photolithography for SU-8 micro-molds; (e) nanoimprinting the PDMS elastic layer with designed microstructures; (f) final package of the sensor.

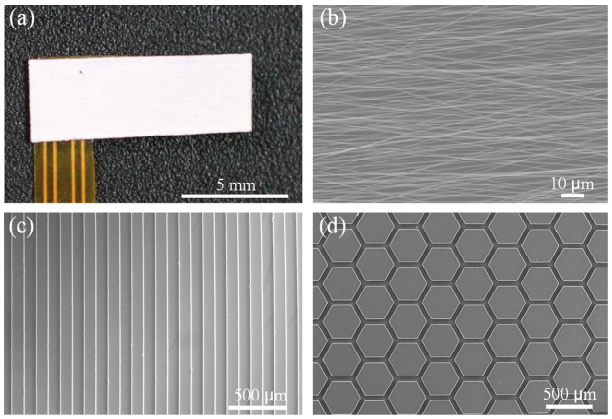

Fig. 5 (a) Photographic image of electrospun P(VDF-TrFE) nanofiber web distributed on lower electrodes; (b) SEM investigation photograph shows highly aligned arrangements of P(VDF-TrFE) nanofibers; (c) parallel ridged microstructures; (d) hexagonal microstructures inspired by human fingertips and tree frog toes pad, respectively.

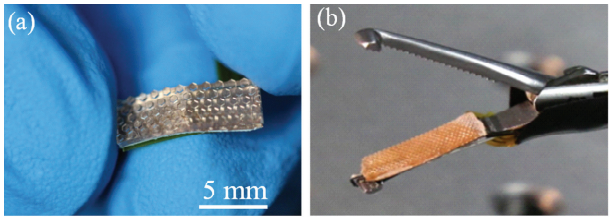

Fig. 6 (a) Photograph of a prototype tactile and slip sensor; (b) a surgical forcep integrated with a tactile and slip sensor.

2.3 Testing procedures

The touch force detection was conducted utilizing a setup as shown in Fig. 7a. The touch force was applied by a single encapsulated piezoelectric actuator (PSt 150/7/100 VS12, Harbin Core Tomorrow Science & Technology Co., Ltd, China) mounted with an aluminium alloy block with a section dimension 10 mm ×5 mm.

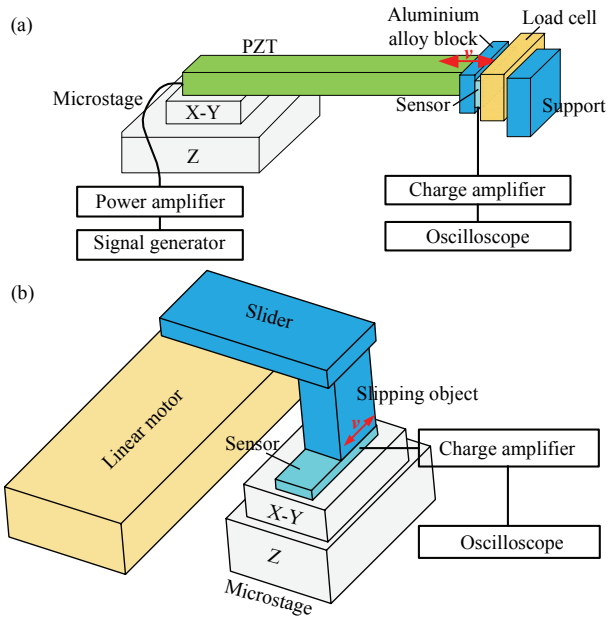

Fig. 7 Schematic illustration of the characterization setups for the tactile and slip sensors. (a) Touch force detection; (b) slip detection.

A function generator (33522A, Agilent, USA) and a power amplifier (XE-50500, Harbin Core Tomorrow Science & Technology Co., Ltd, China) were used to drive the piezoelectric actuator. The touch force applied on the tactile and slip sensor was measured by a load cell (JLWS-5kg, Jinlisensor, China). The signals from sensing elements were amplified by a multi-channel charge amplifier (NEXUS Conditioning Amplifier-2692, Brüel & Kjær, Denmark). Finally, the signals were recorded on a digital oscilloscope (TDS 2012C, Tektronix, USA).

The slip detection was characterized using a measurement setup as shown in Fig. 7b. A linear motor

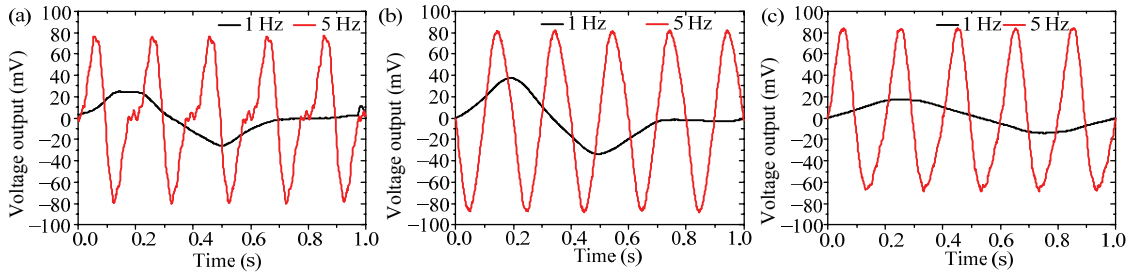

Fig. 8 The voltage outputs of the tactile and slip sensors with different surface structures when applied with sinusoidal excitations at frequencies of 1 Hz and 5 Hz, respectively. (a) The voltage outputs of the sensor without microstructures applied with a peak force of 190 mN; (b) the voltage outputs of the sensor with 400 μm inter-ridge microstructures applied with a peak force of 155 mN; (c) the voltage outputs of the sensor with hexagonal microstructures applied with a peak force of 100 mN.

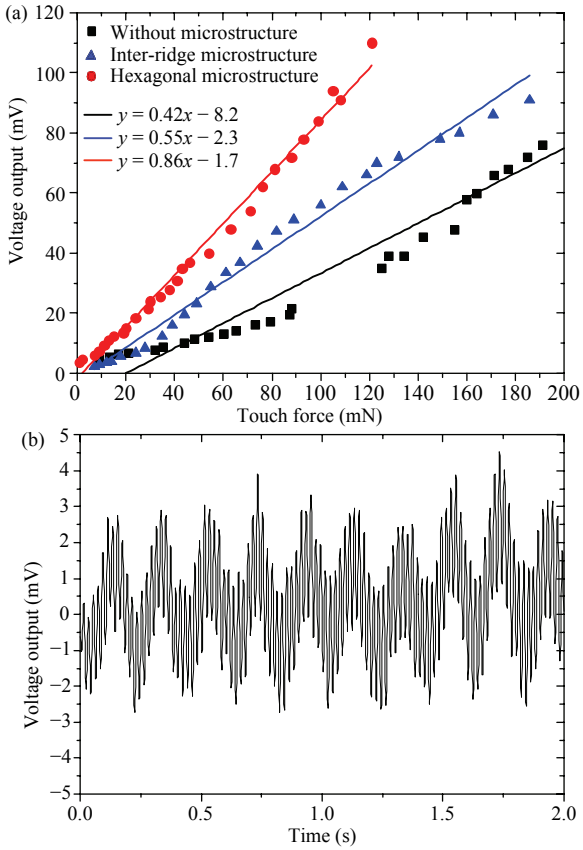

Fig. 9 Characterization of the sensor sensitivity to touch force. (a) The voltage outputs of sensors with different surface structures when applied with a touch excitation at a frequency of 5 Hz; (b) the voltage output of the sensor with hexagonal microstructures when applied with a touch force of 1 mN.

was used to realize a controllable sliding between the slipping object (aluminium alloy block with a section dimension 10 mm × 5 mm) and the sensor surface. The sliding velocity was set to be 2.5 mm·s^{-1} for all the slipping experiments. The signals from the slip sensor units were amplified by the multi-channel charge amplifier. The output signals from the charge amplifier were also recorded using the digital oscilloscope.

3 Characterization results and discussions

3.1 Touch force detection

In order to determine the dynamic sensitivity of the tactile and slip sensor, dynamic touch forces with frequencies of 1 Hz and 5 Hz were applied directly to the sensor surface in the normal direction. When a sinusoidal touch force is applied on the sensor surface in the normal direction, the voltage output of the sensor is also sinusoidal with a frequency identical to the excitation as shown in Fig. 8. For sensors without surface structures, the voltage output of sensors at 5 Hz is much larger than that at 1 Hz with touch forces of 190 mN (Fig. 8a). For sensors with 400 μm inter-ridge microstructures and with hexagonal microstructures (160 μm side length), the voltage outputs are also improved by increasing the frequency (Figs. 8b and 8c). The piezoelectric materials output is positive correlated with its strain rate[34,35]. As the strain rate of P(VDF-TrFE) nanofibers increases with the excitation frequency, the voltage output with 5 Hz excitation is higher than that with 1 Hz excitation.

The characterization results of the sensor sensitivity to touch force are illustrated in Fig. 9. The sensitivity of sensor (the scope of fit lines) without microstructures, with 400 μm inter-ridge microstructures and with hexagonal microstructures (160 μm side length) are 0.42 mV·mN^{-1}, 0.55 mV·mN^{-1} and 0.86 mV·mN^{-1}, respectively. The variation in the sensitivities of the sensors probably originates from stress concentration induced by the microstructures. As the noise level is approximately 2 mV, the minimum dynamic touch force detected by the proposed sensors is as low as 1 mN. The sensor performed much lower detection limit than most

previous works[10,11,14,15] which were based on organic piezoelectric films as show in Table 1.

3.2 Slip detection

Tactile and slip sensors with 400 μm and 800 μm inter-ridge structures were developed. When applied on a touch force in its surface normal direction, the neighboring sensing elements show voltage output without phase differences as shown in Figs. 10a and 11a. When a slip motion appeared on the sensor with 400 μm inter-ridge structures, the output signals of neighboring sensing elements are shown in Fig. 10b, which show a visible phase difference. As the relative slip velocity was 2.5 mm·s^{-1}, the theoretical peak in frequency domain was calculated to be 6.25 Hz. By Fast Fourier Transform (FFT) using the data shown in Fig. 10c, we obtained the outputs in frequency domain with a peak at 5.8 Hz and 6.3 Hz, respectively, which were close to the theoretical results. In the case of 800 μm inter-ridge structures, the slip motion also creates time-domain voltage outputs with a small phase difference as shown in Fig. 11b. The frequency peaks after FFT are both 3.2 Hz for the two neighboring sensing elements as shown in Fig. 11c. The above results suggest that sensor is able to discriminate slip motion from normal tactile force applied on the surface. The periodical surface microstructures can be used to modify the micro-vibration induced by slip motion.

The measurement results using the tactile and slip sensor with hexagonal structures are illustrated in Fig. 12. The side length of the hexagonal microstructure was 320 μm. Touch force induces output signals in the same waveform without phase differences (Fig. 12a). However, the output signals of neighboring sensing elements are quite different from each other in the time domain (Fig. 12b), and the FFT results show frequency peaks at 2.3 Hz and 3.1 Hz (Fig. 12c). The great

Table 1 The comparison of related works on tactile sensors based on flexible organic piezoelectric materials

Author	Year	Functional material	Minimum touch force detected (mN)
Li *et al.*[10]	2008	P(VDF-TrFE) film	25
Qasaimeh *et al.*[11]	2009	PVDF film	10
Dahiya *et al.*[14]	2012	P(VDF-TrFE) film	10
Khan *et al.*[15]	2015	P(VDF-TrFE) film	500
This work	2017	P(VDF-TrFE) nanofibers	1

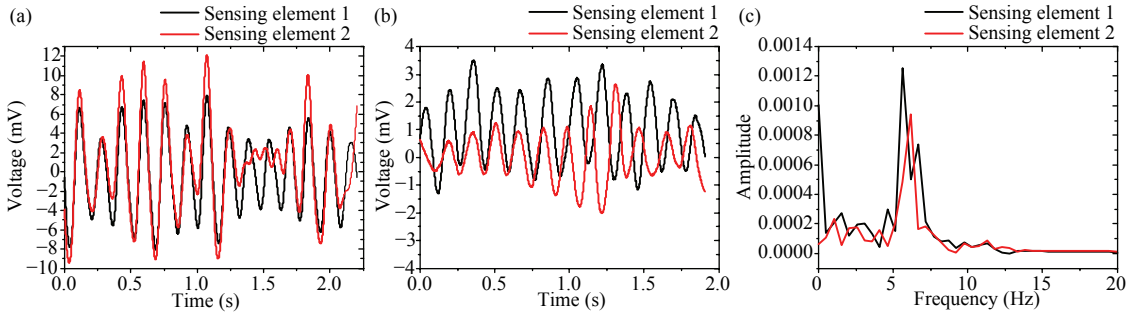

Fig. 10 Touch force and slipping detection using a sensor with 400 μm inter-ridge microstructures. (a) Sensor output when applied with intermittent touch force; (b) sensor output for controlled slipping; (c) FFT results of the sensor output for controlled slipping.

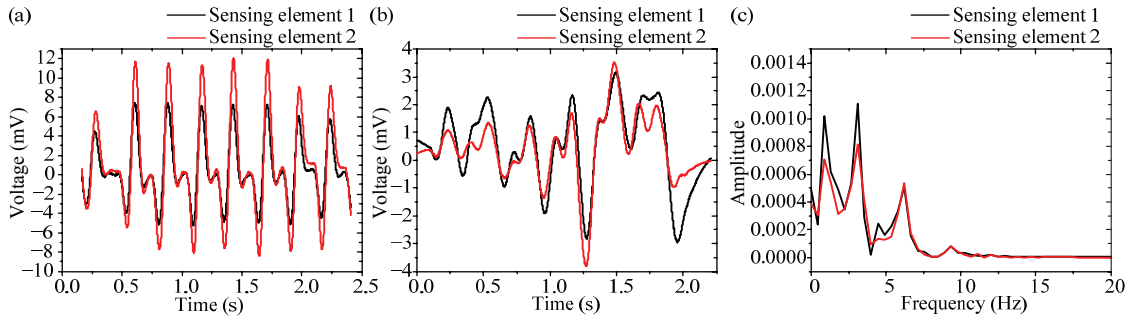

Fig. 11 Touch force and slipping detection using a sensor with 800 μm inter-ridge microstructures. (a) Sensor output when applied with intermittent touch force; (b) sensor output for controlled slipping; (c) FFT results of the sensor output for controlled slipping.

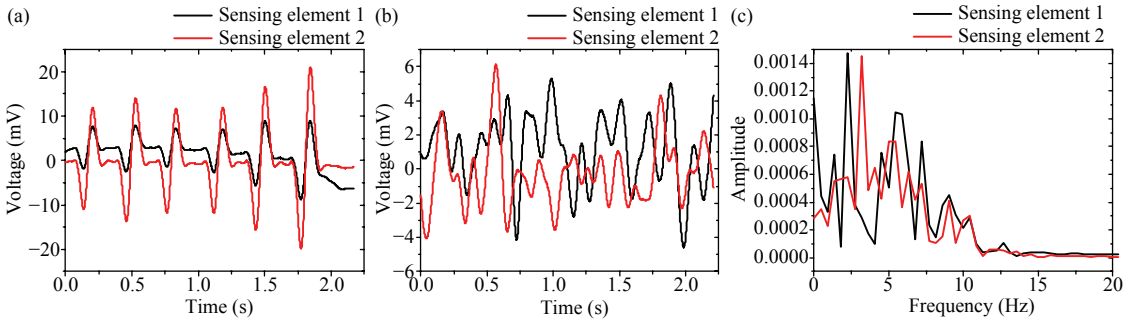

Fig. 12 Touch force and slipping detection for the sensor with hexagonal microstructures. (a) Sensor output when applied with intermittent normal force; (b) sensor output for controlled slipping; (c) FFT results of the sensor output for controlled slipping.

Table 2 Standard deviation of time delay between neighboring sensor units

Surface textures	Standard deviation of time delay for touch force detection (ms)	Standard deviation of time delay for slipping detection (ms)
800 μm inter-ridge microstructures	1.2	14.3
400 μm inter-ridge microstructures	2.4	21.4
320 μm hexagonal microstructures	1.2	36.2

variation in output signals of neighboring sensing elements probably originates from the complex micro-vibrations induced by the hexagonal microstructures.

In order to establish a criterion to discriminate slip motion from repeated touch force using the sensor outputs, we calculated the standard deviation of time delay between the neighboring sensor output signals for five individual periods. As shown in Table 2, in the case of repeated touch forces applied in surface normal indirection, the standard deviation of time delay are all less than 2.4 ms for all the above surface microstructures. However, when the sensors are applied with slip motion, the standard deviations of time delay are 14.3 ms, 21.4 ms and 36.2 ms for 800 μm inter-ridge, 400 μm inter-ridge and hexagonal microstructures, respectively. Herein, the standard deviation of time delay can be used as the criterion to discriminate slip motion from touch forces.

The experimental results showed that the developed sensor also could distinguish slip motion from repeated touch forces utilizing the standard deviation of time delay of the sensor output signals from adjacent sensing elements. It should be addressed that these results are limited to only 2 types of microstructures and the detailed investigation on different microstructures with various dimensions are required for a systematic conclusion.

4 Conclusion

In summary, we developed a bio-inspired tactile and slip sensor comprising of an elastic layer with surface textures, a P(VDF-TrFE) nanofiber web based sensing layer, and a flexible PCB substrate. The proposed sensor was able to perceive both tactile force with a low detection limit (1 mN) and slip motion. It also could discriminate slip motion from repeated touch force using the standard deviation of time delay of the sensor output signals from neighboring sensing elements. As this article is focused on the sensor development and discrimination strategy of tactile force and slip motion, the detailed investigation on microstructures and other experimental issues will be evaluated in the nearby future. However, we believe that this device can play an important part in MIS applications by integrating the sensor into surgical forceps.

Acknowledgment

This work was supported by the National Nature Science Foundation of China (No. 51575027), the Beijing Municipal Natural Science Foundation (No. 3152017), and the Beijing Nova Program (No. Z141104001814035).

References

[1] Stassi S, Cauda V, Canavese G, Pirri C F. Flexible tactile sensing based on piezoresistive composites: A review. *Sensors*, 2014, **14**, 5296–5332.

[2] Kim D, Lu N, Ghaffari R, Kim Y, Lee S P, Xu L, Wu J, Kim R, Song J, Liu Z, Viventi J, de Graff B, Elolampi B, Mansour M, Slepian M J, Hwang S, Moss J D, Won S, Huang Y, Litt B,

Rogers J A. Materials for multifunctional balloon catheters with capabilities in cardiac electrophysiological mapping and ablation therapy. *Nature Materials*, 2011, **10**, 316–323.

[3] Puangmali P, Althoefer K, Seneviratne L D, Murphy D, Dasgupta P. State-of-the-art in force and tactile sensing for minimally invasive surgery. *IEEE Sensors Journal*, 2008, **8**, 371–381.

[4] Eltaib M E H, Hewit J R. Tactile sensing technology for minimal access surgery – A review. *Mechatronics*, 2003, **13**, 1163–1177.

[5] Konstantinova J, Jiang A, Althoefer K, Dasgupta P, Nanayakkara T. Implementation of tactile sensing for palpation in robot-assisted minimally invasive surgery: A review. *IEEE Sensors Journal*, 2014, **14**, 2490–2501.

[6] Zareinia K, Maddahi Y, Gan L S, Ghasemloonia A, Lama S, Sugiyama T, Yang F W, Sutherland G R. A force-sensing bipolar forceps to quantify tool – Tissue interaction forces in microsurgery. *IEEE/ASME Transactions on Mechatronics*, 2016, **21**, 2365–2377.

[7] Althoefer K. Miniature 3-axis distal force sensor for minimally invasive surgical palpation. *IEEE/ASME Transactions on Mechatronics*, 2012, **17**, 646–656.

[8] Núñez C G, Navaraj W T, Polat E O, Dahiya R. Energy-autonomous, flexible, and transparent tactile skin. *Advanced Functional Materials*, 2017, **27**, 1606287.

[9] Narendiran A, George B. Capacitive tactile sensor with slip detection capabilities for robotic applications. 32*nd Annual IEEE Instrumentation and Measurement Technology Conference* (I2MTC), Pisa, Italy, 2015, 464–469.

[10] Li C, Wu P M, Lee S, Gorton A, Schulz M J, Ahn C H. Flexible dome and bump shape piezoelectric tactile sensors using PVDF-TrFE copolymer. *Journal of Microelectromechanical Systems*, 2008, **17**, 334–341.

[11] Qasaimeh M A, Sokhanvar S, Dargahi J, Kahrizi M. PVDF-based microfabricated tactile sensor for minimally invasive surgery. *Journal of Microelectromechanical Systems*, 2009, **18**, 195–207.

[12] Dargahi J, Sedaghati R, Singh H, Najarian S. Modeling and testing of an endoscopic piezoelectric-based tactile sensor. *Mechatronics*, 2007, **17**, 462–467.

[13] Wang Y R, Zheng J M, Ren G Y, Zhang P H, Xu C. A flexible piezoelectric force sensor based on PVDF fabrics. *Smart Materials and Structures*, 2011, **20**, 045009.

[14] Dahiya R S, Adami A, Collini C, Lorenzelli L. POSFET tactile sensing arrays using CMOS technology. *Procedia Engineering*, 2012, **47**, 894–897.

[15] Khan S, Tinku S, Lorenzelli L. Flexible tactile sensors using screen-printed P(VDF-TrFE) and MWCNT/PDMS composites. *IEEE Sensors Journal*, 2015, **15**, 3146–3155.

[16] Yi Z, Zhang Y. Bio-inspired tactile FA-I spiking generation under sinusoidal stimuli. *Journal of Bionic Engineering*, 2016, **13**, 612–621.

[17] Okatani T, Takahashi H, Noda K, Takahata T. A tactile sensor using piezoresistive beams for detection of the coefficient of static friction. *Sensors*, 2016, **16**, 718.

[18] Prasad S K, Kitagawa M, Fischer G S, Zand J, Talamini M A, Taylor R H, Okamura A M. A modular 2-DOF force-sensing instrument for laparoscopic surgery. *International Conference on Medical Imaging Computing and Computer-Assisted Intervention*, Montreal, Canada, 2003, 279–286.

[19] Wang X, Sun Y, Wang Y, Hu T, Chen M, He B. Artificial tactile sense technique for predicting beef tenderness based on FS pressure sensor. *Journal of Bionic Engineering*, 2009, **6**, 196–201.

[20] Someya T, Kato Y, Sekitani T, Iba S, Noguchi Y, Murase Y, Kawaguchi H, Sakurai T. Conformable, flexible, large-area networks of pressure and thermal sensors with organic transistor active matrixes. *Proceedings of the National Academy of Sciences of the United States of America*, 2005, **102**, 1–5.

[21] Lim S, Lee H, Park J. Grip force measurement of forceps with fibre Bragg grating sensors. *Electronics Letters*, 2014, **50**, 733–735.

[22] Ahmadi R, Packirisamy M, Dargahi J, Cecere R. Discretely loaded beam-type optical fiber tactile sensor for tissue manipulation and palpation in minimally invasive robotic surgery. *IEEE Sensors Journal*, 2012, **12**, 22–32.

[23] Iii F L H, Kramer R K, Wan Q, Howe R D, Wood R J. Soft tactile sensor arrays for force feedback in micromanipulation. *IEEE Sensors Journal*, 2014, **14**, 1443–1452.

[24] Liu Y, Han H, Liu T, Yi J, Li Q, Inoue Y. A novel tactile sensor with electromagnetic induction and its application on stick-slip interaction detection. *Sensors*, 2016, **16**, 430.

[25] Ahmed M, Chitteboyina M M, Butler D P, Çelik-butler Z. MEMS force sensor in a flexible substrate using nichrome piezoresistors. *IEEE Sensors Journal*, 2013, **13**, 4081–4089.

[26] Francomano M T, Accoto D, Guglielmelli E. Experimental characterization of a flexible thermal slip sensor. *Sensors*, 2012, **12**, 15267–15280.

[27] Fernandez R, Payo I, Vazquez A S, Becedas J. Micro-vibration-based slip detection in tactile force sensors. *Sensors*, 2014, **14**, 709–730.

[28] Zhang X, Liu R. Slip detection by array-type pressure sensor

for a grasp task. *In Proceedings of* 2012 *IEEE International Conference on Mechatronics and Automation*, Chengdu, China, 2012, 2198–2202.

[29] Scheibert J, Leurent S, Prevost A, Debrégeas G. The role of fingerprints in the coding of tactile information probed with a biomimetic sensor. *Science*, 2009, **323**, 1503–1506.

[30] Chen H, Zhang L, Zhang D, Zhang P, Han Z. Bioinspired surface for surgical graspers based on the strong wet friction of tree frog toe pads. *ACS Applied Materials & Interfaces*, 2015, **7**, 13987–13995.

[31] Jiang Y G, Shiono S, Hamada H, Fujita T, Zhang D Y, Maenaka K. Reactive ion etching of poly(vinylidene fluoride-trifluoroethylene) copolymer for flexible piezoelectric devices. *Chinese Science Bulletin*, 2013, **58**, 2091–2094.

[32] Jiang Y G, Gong L L, Hu X H, Zhao Y, Chen H W, Feng L, Zhang D Y. Aligned P(VDF-TrFE) nanofibers for enhanced piezoelectric directional strain sensing. *Polymers*, 2018, **10**, 364.

[33] Persano L, Dagdeviren C, Su Y, Zhang Y, Girardo S, Pisignano D, Huang Y, Rogers J A. High performance piezoelectric devices based on aligned arrays of nanofibers of poly(vinylidenefluoride-co-trifluoroethylene). *Nature Communications*, 2013, **4**, 1633.

[34] Sirohi J, Chopra I. Fundamental understanding of piezoelectric strain sensors. *Journal of Intelligent Material Systems and Structures*, 2000, **11**, 246–257.

[35] Pan C T, Yen C K, Wang S Y, Lai Y C, Lin L, Huang J C, Kuo S W. Near-field electrospinning enhances the energy harvesting of hollow PVDF piezoelectric fibers. *RSC Advances*, 2015, **5**, 85073–85081.